Applied Physics A (2020) 126:649
https://doi.org/10.1007/s00339-020-03853-3

Applied Physics A
Materials Science & Processing

Ultrafast laser ablation of copper by GHz bursts

Chung-Wei Cheng[1] · **Jinn-Kuen Chen**[2]

Received: 28 March 2020 / Accepted: 24 July 2020 / Published online: 31 July 2020

Abstract
The ablation of copper, using a 10 GHz burst ultrafast laser with a wavelength of 1030 nm, a pulse duration of 1 ps, a variable total laser fluence, and a number of sub-pulses per burst, is investigated theoretically. A two-temperature model with an extended Lorentz–Drude model for dynamic optical properties is used to simulate the melting and ablation process. Due to the heat accumulation from the preceding pulses, multipulse laser ablation could be advantageous over a single pulse. Moreover, the ablation performance can be maximized by properly selecting the pulse number, separation time, and energy in a laser burst. The numerical result shows that the present prediction is in fairly agreement with existing experimental result. Under the same total laser fluence of 32 J/cm^2, a 10 GHz burst laser with an optimized 128 sub-pulse can significantly enhance the ablation depth, 4.2 times that a single pulse does. It is found that the optimized ablation depth is a linear function of the total fluence of ultrafast laser bursts.

Keywords Ultrafast laser · GHz burst · Two-temperature model

1 Introduction

Ultrafast lasers have been applied in the internal modification of transparent material and surface structuring of opaque material because of their high peak power intensity [1] and minimal heat-affected zone (HAZ) [2]. The repetition rates of the ultrafast laser source usually range from kHz to MHz, and recently to GHz. When processing a metal using an ultrafast laser with a kHz repetition rate, phase explosion is one of the ablation mechanisms, and the overheated liquid metal relaxes explosively (or sputters) into a mixture of vapors that is immediately ejected from the bulk metal [3, 4]. When processing a metal by an ultrafast laser with MHz bursts, the heat accumulation effect and obvious HAZ can be found in the process since the sub-pulse separation time (1 μs for 1 MHz) is usually much shorter than the effective cooling time (i.e. tens of μs) of the metal [5].

When a laser source has ultrafast GHz burst characteristics, the pulse duration and the repetition rate for the sub-pulses in the bursts are ultrafast (ps or fs) and GHz, respectively. Recently, numerous experiments on material ablation using ultrafast lasers with GHz bursts have been presented for metals [6–8] and silicon [9]. The sub-pulse laser fluence of each pulse considered is usually below the ablation threshold. It is interesting that the cool material ablation can occur when the separation time of the sub-pulses within a burst, e.g. 1 ns for 1 GHz, is less than the thermal relaxation time of the material, e.g. 1.1 ns for Cu [6]. A two-stage mechanism for GHz burst ablation was recently proposed by [7]. The first-stage is heating the material to a liquid state by accumulation effects, and the second-stage is effective ablation of the hot surface layer. Percussion drilling on Cu using an ultrafast laser with 0.864–3.52 GHz bursts was presented in [7, 8]. However, HAZ was found experimentally, and the authors claimed that the true "ablation cooling" effect is not presented.

In our previous study [10], ablation of Cu by ultrafast bursts was investigated theoretically. Different repetition rates of 2–1000 GHz for sub-pulses in the bursts, different sub-pulse numbers 1–10 and a total fluence of 10 J/cm^2 were investigated. The maximum ablation depth obtained was found by the 10 GHz rate and sub-pulse number 6. The fluence of each pulse, 1.67 J/cm^2, was higher than

✉ Chung-Wei Cheng
weicheng@nctu.edu.tw

[1] Department of Mechanical Engineering, National Chiao Tung University, No. 1001, Ta Hsueh Road, Hsinchu 30010, Taiwan

[2] Department of Mechanical and Aerospace Engineering, University of Missouri, Columbia, MO 65211, USA

the material's ablation threshold of 0.6 J/cm^2. However, the modeling of the metal ablation by GHz bursts with a fluence of each pulse below the ablation threshold was not investigated. In addition, the optimized sub-pulse number for a burst with a fixed total fluence and small HAZ was not presented.

In this study, the optimal ablation of copper by an ultrafast laser with 10 GHz bursts is investigated using a computational model. The numerical results of the optical, thermal, and the melting and ablation depth responses under different total laser fluences and sub-pulse numbers are discussed herein.

2 Modeling

A copper material is irradiated by a GHz burst ultrafast laser on the surface ($z=0$), and the laser beam is propagated along the z-axis. A numerical model was performed based on our previous study [10] and the ballistic electron penetration depth is considered in this study. The main modules included a two-temperature model, an optical model, phase change models, and phase explosion model. The laser heat density for a burst laser can be expressed as:

$$S(z,t)=\sum_{i=1}^{M}\sum_{j=1}^{N}0.94\frac{[1-R(0,t)]F_{ij}}{t_\mathrm{p}}\frac{1}{\delta(z,t)+\delta_\mathrm{b}}\exp\left[-\int_0^z\frac{1}{\delta(z,t)+\delta_\mathrm{b}}\mathrm{d}z-2.77\left(\frac{t-\frac{i-1}{f_\mathrm{rep}}-(j-1)t_\mathrm{sep}}{t_\mathrm{p}}\right)^2\right], \quad (1)$$

where M is the number of laser bursts, N is the number of sub-pulses in the burst, F_{ij} is the sub-pulse laser fluence of the j-pulse in the i-burst, t_sep is the sub-pulse separation time, f_rep is the burst repetition rate, t_p is the sub-pulse duration, $R(0,t)$ is the surface reflectivity of the material at $z=0$, $\delta(z,t)=1/\alpha(z,t)$ is the optical penetration depth, and δ_b is the ballistic motion of the photon-excited hot electrons. The inclusion of δ_b alters the distribution of laser energy penetration into the material, and thereby could result in different temperature distribution. In this study, all the sub-pulse laser fluences are identical, i.e. $F_{ij}=F_\mathrm{p}$, and $\delta_\mathrm{b}=15$ nm for copper is used [11]. Figure 1 depicts a single pulse and two laser pulse trains consisting of $N=3$ and $N=6$ pulses with $t_\mathrm{sep}=100$ ps and the same total fluence.

The temperature-dependent dynamic optical properties of $R(0,t)$ and $\delta(z,t)$ could significantly alter the laser energy absorption and, in turn, influence the distribution of laser heat density. In [10], the critical point model with three Lorentzian terms was used to calculate the dynamic optical properties. To simplify the calculation, an extended Lorentz–Drude model [12, 13] is used in this study:

$$\varepsilon(\omega)=\varepsilon_\infty-\frac{\omega_\mathrm{p}^2}{\omega_\mathrm{L}^2+i\gamma_\mathrm{D}\omega}-\frac{f\Omega_\mathrm{L}^2}{\left(\omega_\mathrm{L}^2-\Omega_\mathrm{L}^2\right)+iA\gamma_\mathrm{D}\omega_\mathrm{L}}=\varepsilon_1+i\varepsilon_2, \quad (2)$$

where ε_∞ is the dielectric constant,ω_L is the laser frequency,ω_p is the plasma frequency, Ω_L represents the oscillator strength of the Lorentz oscillators, f is a weighting factor, A is a constant, and γ_D is the damping coefficient. $\gamma_\mathrm{D}=1/\tau_\mathrm{e}$, where τ_e is the electron relaxation time. The following values are optimized for copper: $\varepsilon_\infty=9.4286$, $\omega_\mathrm{p}=1.3593\times10^{16}$ Hz, $\Omega_\mathrm{L}=1.7668\times10^{15}$ Hz, $f=3.6355$, and $A=44.5275$. The laser frequency $\omega_\mathrm{L}=1.829\times10^{15}$ rad/s for a laser wavelength of $\lambda=1030$ nm.

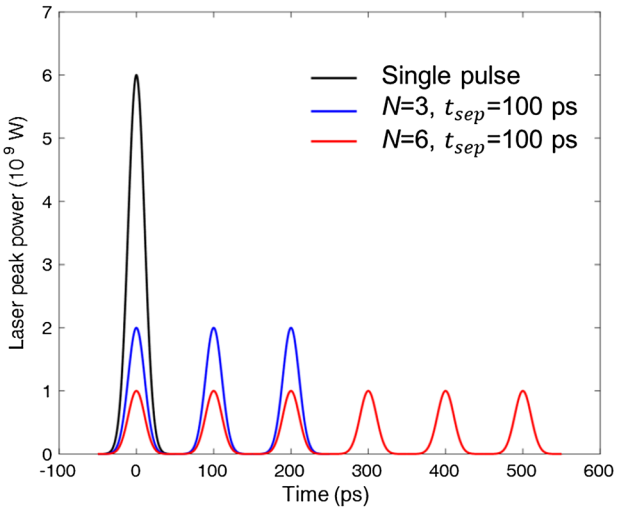

Fig. 1 A single laser pulse and two pulse trains consisting of $N=3$ and 6 pulses with $t_\mathrm{sep}=100$ ps and the same total fluence

3 Results and discussion

Copper, with an initial temperature of 300 K, was irradiated on its front surface by a laser burst with 10 GHz ($t_\mathrm{sep}=100$ ps), $t_\mathrm{p}=1$ ps, and $\lambda=1030$ nm. The single-shot ablation threshold fluence F_th of the Cu was determined to be about $F_\mathrm{th}=0.6$ J/cm^2. The threshold value was determined by setting the simulated ablation depth near zero. The simulated ablation threshold fluence is slightly smaller than the experimental values, e.g. about 0.7 J/cm^2 by laser (1030 nm, 1 ps) [14].

Figure 2 compares the calculated optical reflectivity (R) and lattice temperature on the copper surface, respectively, for a two-pulse burst of sub-pulse fluences $F_\mathrm{p}=0.5$ J/cm^2 with and without the δ_b. It is shown in Fig. 2a that the

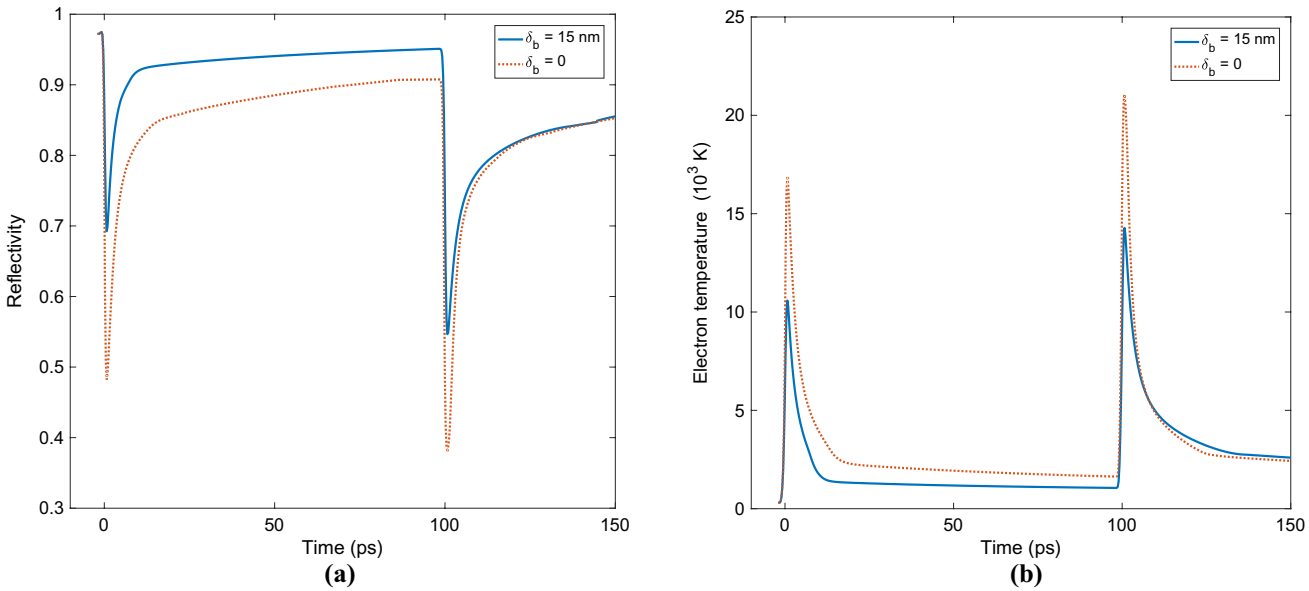

Fig. 2 Time dependence of calculated **a** surface reflectivity and **b** electron temperature for a two-pulse burst of sub-pulse fluences 0.5 J/cm^2 with and without the δ_b

inclusion of δ_b results in a higher R. The increase in R causes the material to absorb less laser energy, leading to lower electron temperature, as shown in Fig. 2b. It should be noted that the inclusion of δ_b could change material absorption for the first laser pulse, and also for the subsequent pulses in addition to the incubation effect.

Two laser bursts, with the same total fluence 5 J/cm^2 and different numbers of sub-pulses $N=6$ and 20, are used to process the Cu. The sub-pulse fluences F_p are 0.833 J/cm^2 and 0.25 J/cm^2, which are higher and lower than the F_{th}, respectively. Figures 3, 4, and 5 show the time dependence of the calculated electron temperature (T_e) and lattice temperature (T_l), reflectivity (R) and optical penetration depth (δ), and ablation depth and liquid–vapor interfacial temperature (T_{lv}), respectively.

In Fig. 3a, for each $F_p > F_{th}$, it is evident that the maximum T_l remains at around 6926 K, i.e. 90% of the critical temperature T_{tc} (7696 K), which is attributed to the phase

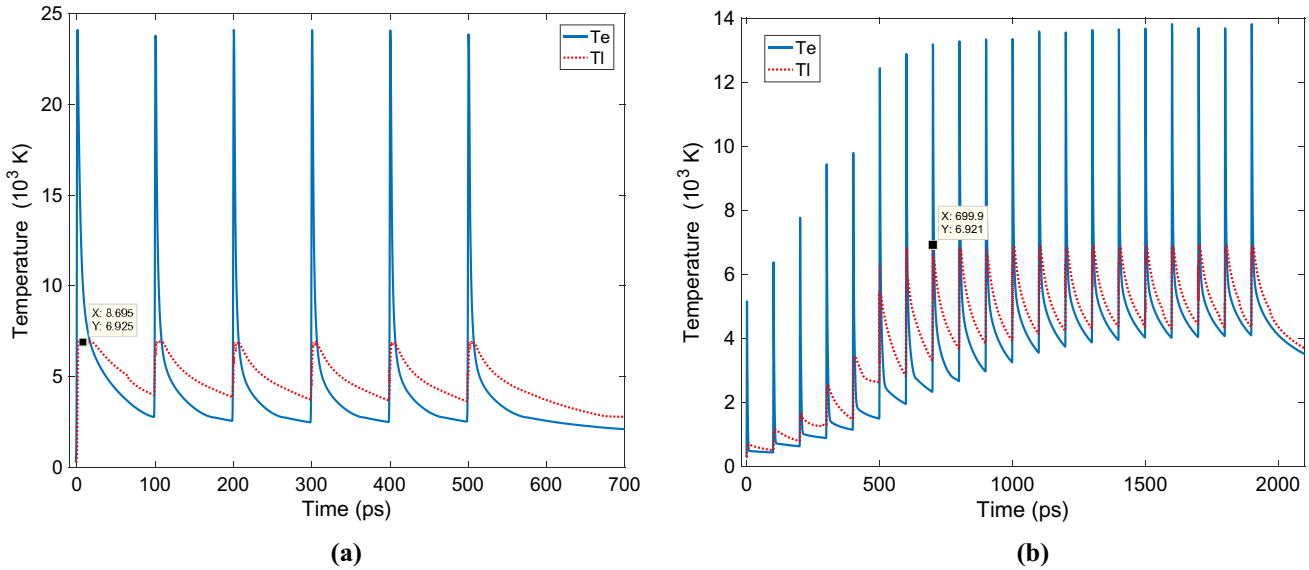

Fig. 3 Time dependence of calculated T_e and T_l by two laser bursts with the same total laser fluence 5.0 J/cm^2 and different pulse numbers **a** $N=6$ and **b** $N=20$

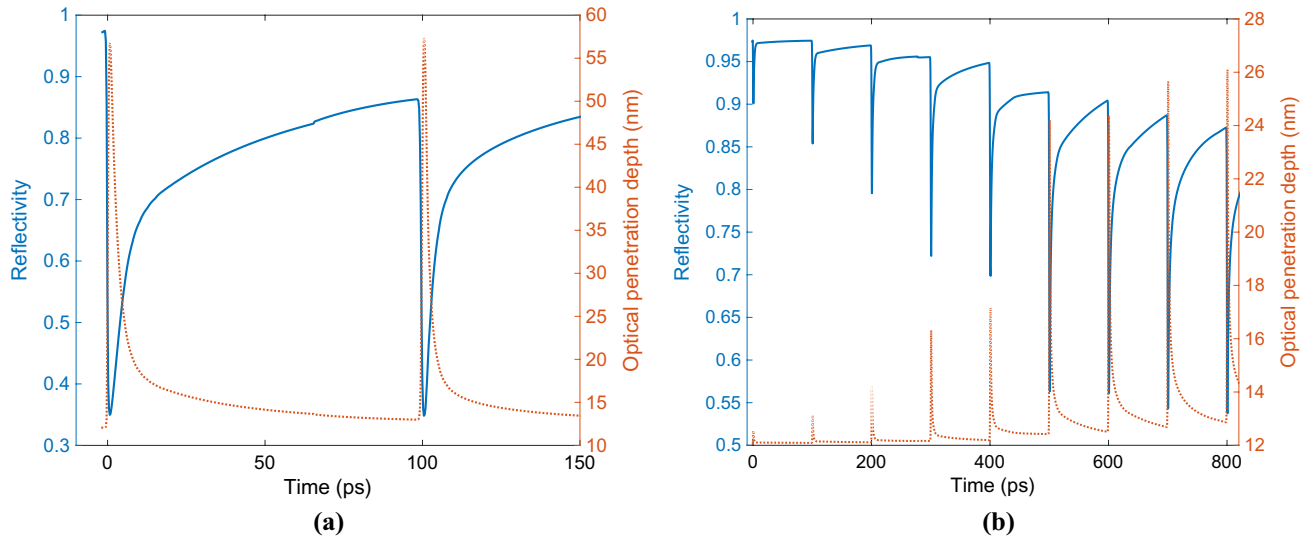

Fig. 4 Time dependence of calculated reflectivity (R) and optical penetration depth (δ) by two laser bursts with the same total laser fluence 5.0 J/cm^2 and different pulse numbers **a** $N=6$ and **b** $N=20$

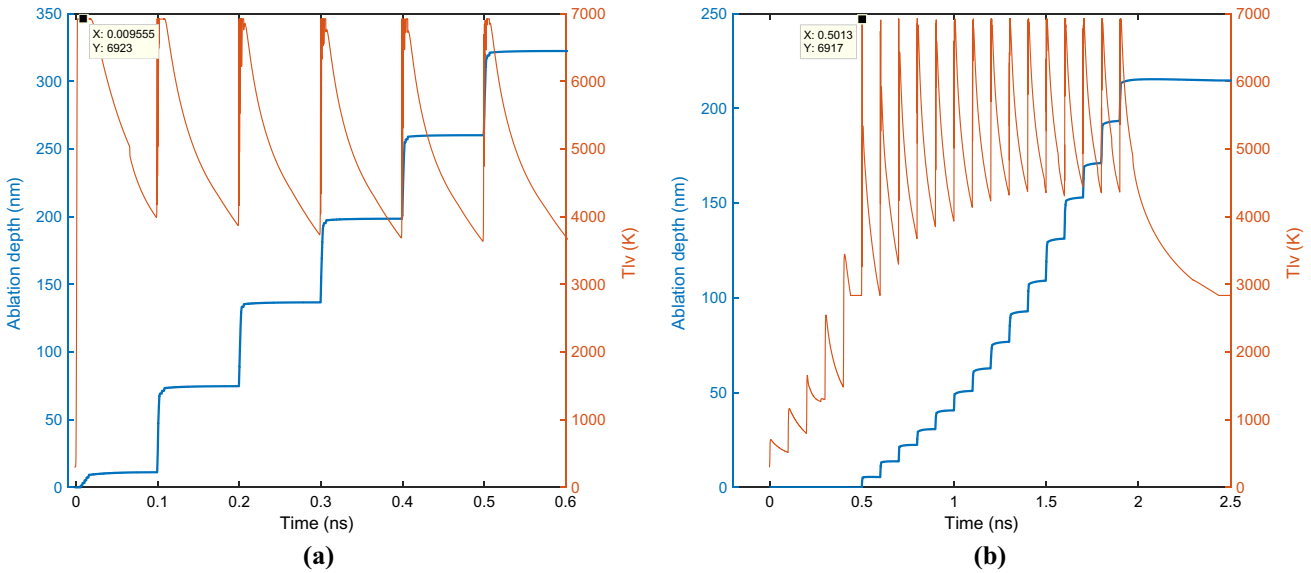

Fig. 5 Time dependence of calculated ablation depth and liquid–vapor interfacial temperature (T_{lv}) by two laser bursts with the same total laser fluence 5.0 J/cm^2 and different pulse numbers **a** $N=6$ and **b** $N=20$

explosion [15]. On the other hand, as shown in Fig. 3b, for each $F_p < F_{th}$, the maximum T_e and T_l gradually increased at each pulse irradiation and the maximum T_l remains at around 6,926 K for $N=8$–20, which is also attributed to the phase explosion. The T_l is heated up via the electron–phonon collisions and decreases from heat diffusion loss until the next pulse starts. For example, the T_l increases from 300 to 705 K after the first pulse irradiation and then decreases to 516 K (at time 98 ps). The T_l increases step-by-step after each pulse irradiation by the heat accumulation effect and reaches 3299 K (at 698 ps) before the 8-pulse (at time 700 ps) irradiation.

In Fig. 4a, for a burst consisting of 6 pulses, the reflectivity R on the surface decreases quickly during the laser pulse irradiation and then increases after the irradiation is over. The δ increases quickly during the laser pulse irradiation and then decreases after the pulse is off. The R at room temperature is 0.97 and decreases to a minimum 0.35 after the 1-pulse irradiation and then increases to 0.86 at time 98 ps. The δ which is 12.1 nm at room temperature increases

to a maximum 56.8 nm and then decreases to 13.0 nm at time 98 ps. On the contrary, for the 20-pulse burst, the minimum R gradually decreases and reaches around 0.54 at the 8-pulse, as shown in Fig. 4b. The decrease in R causes the material to absorb more laser fluence. With the increase in δ, the laser heat density distribution inside the target will become deeper.

In Fig. 5a, for the 6-pulse burst, ablation occurs after the first pulse irradiation. The repeating steep occurrences of material ablation right after the second pulse result mainly from the phase explosion, while the flatter one is from vaporization. The final ablation depth is about 322 nm at time 0.6 ns. The maximum T_{lv} reaches $0.9T_{tc}$ after each pulse irradiation. When the superheated liquid reaches $0.9T_{tc}$, that matter is removed via phase explosion [15]. At this state, the superheated liquid relaxes explosively into a mixture of vapor and droplets that are ejected from the irradiated material, and the nanoparticles was deposited around the ablation crater [3].

On the other hand, for the 20-pulse burst, ablation begins from the 6th pulse (at time 0.5 ns) and the final ablation depth is 215 nm at time 2.5 ns, as shown in Fig. 5b. The T_{lv} increases step-by-step after each pulse irradiation by the heat accumulation effect; but, the ablation does not take place because the peak lattice temperature nearly reaches the normal boiling point. When the 6th pulse (at time 0.5 ns) irradiates on a hot surfaced layer, the maximum T_{lv} reaches $0.9T_{tc}$ and, thus, ablation starts. It is found that with a fixed total laser fluence, the ablation depth generated by a 6-pulse burst is about 1.5 times that by a 20-pulse burst. This suggests that the sub-pulse number (N) and fluence (F_p) in a burst are important parameters, resulting in different total ablation depths.

Figure 6 shows the ablation and melting depths of the Cu processed by two laser bursts with $N=6$ ($F_p \sim 0.833$ J/cm^2) and $N=14$ ($F_p \sim 0.357$ J/cm^2), in which the total fluences are the same as for 5 J/cm^2. It appears that the melting depths are quite different although the ablation depths are similar for the two kinds of bursts, i.e. about 323 nm. For the 6-pulse burst case, a phase explosion occurs right after the impinging of each subsequent laser pulse as aforementioned. The ablation depth of each pulse was mainly controlled by the optical penetration depth of the material. The HAZ (the difference between the melting and ablation depth) was small, i.e. about 90 nm. On the other hand, for the 14-pulse burst case, ablation begins after the 3-pulse (at time 200 ps). It was evident that the HAZ grows thicker and thicker after the subsequent pulse irradiates. The final ablation depth is about 323 nm (at time 1500 ps) while the melting depth reaches 521 nm, and HAZ is about 198 nm.

In the GHz burst ultrafast laser ablation process, it is desirable that the maximum ablation depth can be obtained and that the HAZ is as low as possible. Figure 7 shows the

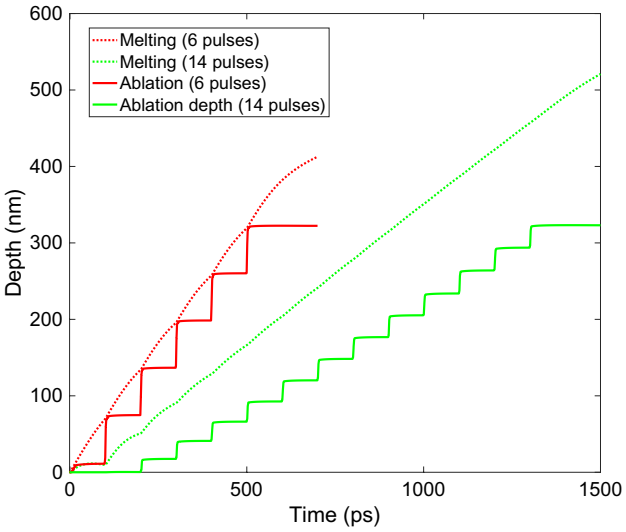

Fig. 6 Ablation and melting depths of the Cu processed by two laser bursts consisting of 6 and 14 pulses with the same total laser fluence of 5.0 J/cm^2

ablation depth, melting depth, and HAZ of the Cu processed by the two laser bursts of total fluence 5 J/cm^2 and 32 J/cm^2 and the number of N in the range 1–40. In Fig. 7a for the 5 J/cm^2 bursts, when $N<8$, both the ablation depth and the HAZ increase with the increase in N. Apparently, the 8-pulse burst ($F_p \sim 1.1\ F_{th}$) achieve the maximum ablation depth of 346 nm, which is 1.8 times more effective than the single-pulse ablation. For $N>8$, the ablation depth tended to decrease and the HAZ tended to increase with the increase in N. The reason for the reduction in ablation depth may be due to less F_p in each pulse resulting in lower T_e and T_l values, and a higher R that reflects more laser energy away. The less F_p that is absorbed, the less material that is ablated. A copper milling by a laser burst with $t_{sep}=180$ ps was reported in [16], where a higher number of pulses per burst lead to an increased melt ejection, which is similar to our simulation results. In Fig. 7b for the 32 J/cm^2 bursts, the maximum ablation depth is achieved by the 128-pulse burst ($F_p \sim 1.1\ F_{th}$), which is 4.2 times that of a single pulse.

The above results demonstrate that an optimum combination of the number the sub-pulses and their fluence for enhancing the ablation efficiency exist. When F_p is slightly higher than the threshold, the ablation is very close to a maximum efficiency, leading to a significant ablation of material while the HAZ remains mild.

Figure 8 compares the total ablation depth between the single pulse and burst over a total fluence of 5–32 J/cm^2. For the laser bursts, the sub-pulse number N in each burst have been optimized for all different total laser fluences. It is interesting to note that the straight lines curve-fitted from the calculated data show the linear dependence between the maximum ablation depth and the total fluence.

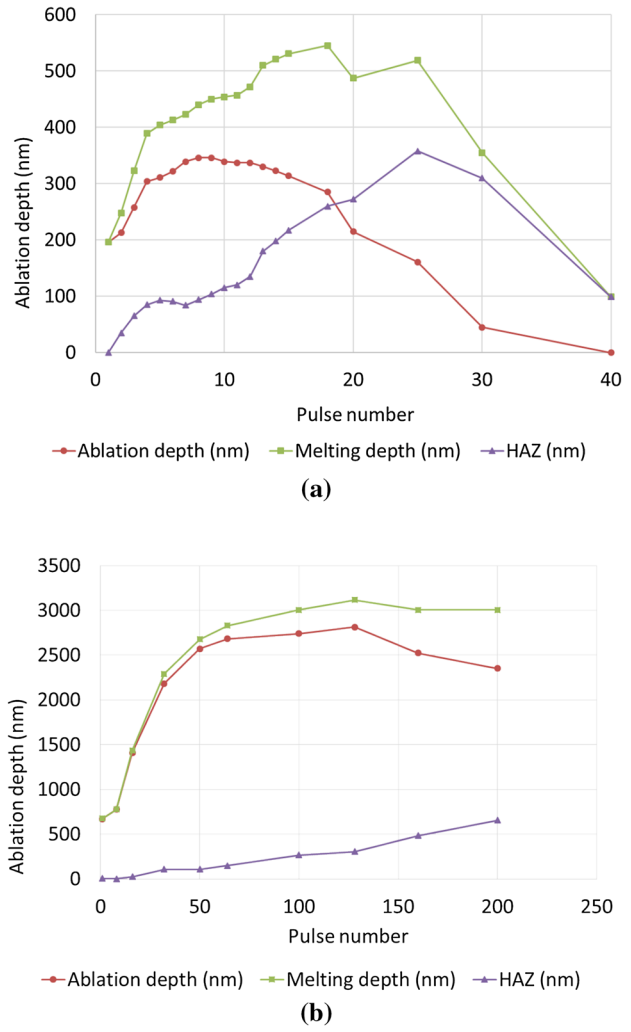

Fig. 7 Ablation by laser bursts having the same total fluence of **a** 5 J/cm^2 and **b** 32 J/cm^2 and N in the range 1–40

Recently, the experimental results for copper percussion drilling by a 1.76 GHz burst femtosecond laser with a total energy of 88 μJ and $N = 200$ was presented in [17]. The ablation depth and burr height around the hole are determined to be about 4 μm and 0.6 μm, respectively. The total fluence is 38.9 J/cm^2 calculated by the total energy of 88 μJ and focused beam diameter of 24 μm (at 1/e^2) presented in [7]. The predicted ablation depth can be computed using the fitting equation, shown in Fig. 8. The estimated ablation depth for fluence 38.9 J/cm^2 is 3.43 μm, which is close to the experimental value of 4 μm in [17]. The total fluence, 38.9 J/cm^2, is slightly higher than the 32 J/cm^2 in Fig. 7b. The simulated HAZ for $N = 200$ in Fig. 7b is 0.67 μm, which is also close to the experimental value of 0.6 μm in [17].

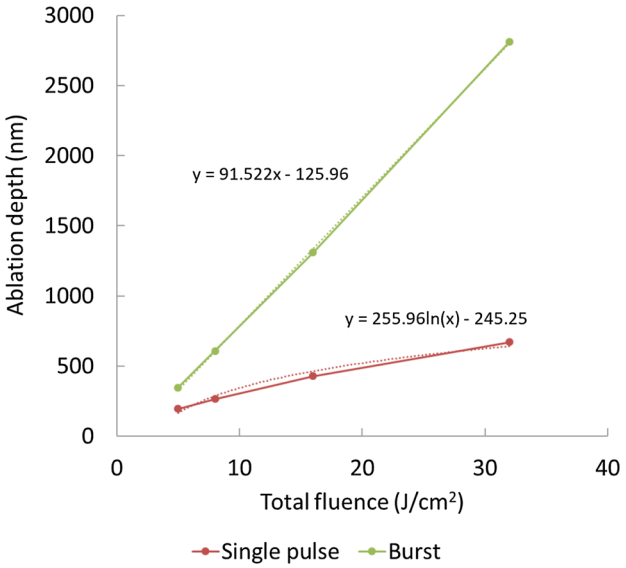

Fig. 8 Comparison of the ablation depths between single pulse and optimized bursts with the same total laser fluences

4 Conclusions

This study presents the numerical results of material ablation of Cu by an ultrafast 10 GHz laser bursts. To simulate the ultrafast GHz laser heating process, a two-temperature model with an extended Lorentz–Drude model for dynamic optical properties and ballistic electron penetration depth in laser heat density, was presented. It is found that a burst laser with a total laser fluence of 5 J/cm^2 and the sub-pulse number 8 can increase the amount of material ablated by 1.8 times, as compared to a single pulse. As the total laser fluence further increases to 32 J/cm^2, the ablation efficiency becomes 4.2 times that of a single pulse. It is demonstrated that an optimized laser burst in terms of the sub-pulse number and fluence for enhancing the ablation efficiency exist. When the sub-pulse fluence is slightly higher than the threshold, the maximum ablation efficiency can be achieved and the HAZ remains mild. The present numerical prediction matches fairly well with existing experimental results. Most importantly, the present study attain a new finding that the optimized ablation depth is a linear function of the total fluence of ultrafast laser bursts.

Acknowledgements This work was supported by the Ministry of Science and Technology of Republic of China, under Contract MOST 107-2221-E-009-061-MY3.

References

1. R.R. Gattass, E. Mazur, Femtosecond laser micromachining in transparent materials. Nat. Photonics **2**, 219–225 (2008)

2. S. Nolte, C. Momma, H. Jacobs, A. Tunnermann, B.N. Chichkov, B. Wellegehausen, H. Welling, Ablation of metals by ultrashort laser pulses. J Opt Soc Am B Opt Phys **14**, 2716–2722 (1997)
3. K.-H. Leitz, B. Redlingshöfer, Y. Reg, A. Otto, M. Schmidt, Metal Ablation with short and ultrashort laser pulses. Phys. Proc. **12**, 230–238 (2011)
4. C.W. Cheng, S.Y. Wang, K.P. Chang, J.K. Chen, Femtosecond laser ablation of copper at high laser fluence: Modeling and experimental comparison. Appl. Surf. Sci. **361**, 41–48 (2016)
5. A. Ancona, S. Döring, C. Jauregui, F. Röser, J. Limpert, S. Nolte, A.J.O.L. Tünnermann, Femtosecond and picosecond laser drilling of metals at high repetition rates and average powers. Opt. Lett. **34**, 3304–3306 (2009)
6. C. Kerse, H. Kalaycıoğlu, P. Elahi, B. Çetin, D.K. Kesim, Ö. Akçaalan, S. Yavaş, M.D. Aşık, B. Öktem, H. Hoogland, R. Holzwarth, F.Ö. Ilday, Ablation-cooled material removal with ultrafast bursts of pulses. Nature **537**, 84–88 (2016)
7. G. Bonamis, K. Mishchick, E. Audouard, C. Hönninger, E. Mottay, J. Lopez, I. Manek-Hönninger, High efficiency femtosecond laser ablation with gigahertz level bursts. J. Laser Appl. **31**, 022205 (2019)
8. Z. Lin, H. Matsumoto, J. Kleinert, Ultrafast laser ablation of copper with~ GHz bursts, in: Laser Applications in Microelectronic and Optoelectronic Manufacturing (LAMOM) XXIII, International Society for Optics and Photonics, pp. 1051902 (2018)
9. K. Mishchik, G. Bonamis, J. Qiao, J. Lopez, E. Audouard, E. Mottay, C. Hönninger, I.J.O.L. Manek-Hönninger, High-efficiency femtosecond ablation of silicon with GHz repetition rate laser source. Opt. Lett. **44**, 2193–2196 (2019)
10. Y. Ren, C.W. Cheng, J.K. Chen, Y. Zhang, D.Y. Tzou, Thermal ablation of metal films by femtosecond laser bursts. Int. J. Therm. Sci. **70**, 32–40 (2013)
11. J. Byskov-Nielsen, J.-M. Savolainen, M.S. Christensen, P. Balling, Ultra-short pulse laser ablation of copper, silver and tungsten: experimental data and two-temperature model simulations. Appl. Phys. A Mater. Sci. Process. **103**, 447–453 (2011)
12. Y.P. Ren, J.K. Chen, Y.W. Zhang, J. Huang, Ultrashort laser pulse energy deposition in metal films with phase changes. Appl. Phys. Lett. **98**, 191105 (2011)
13. G.D. Tsibidis, The influence of dynamical change of optical properties on the thermomechanical response and damage threshold of noble metals under femtosecond laser irradiation. J. Appl. Phys. **123**, 085903 (2018)
14. P.T. Mannion, J. Magee, E. Coyne, G.M. O'Connor, T.J. Glynn, The effect of damage accumulation behaviour on ablation thresholds and damage morphology in ultrafast laser micro-machining of common metals in air. Appl. Surf. Sci. **233**, 275–287 (2004)
15. R. Kelly, A. Miotello, Comments on explosive mechanisms of laser sputtering. Appl. Surf. Sci. **96–98**, 205–215 (1996)
16. T. Hirsiger, M. Gafner, S. Remund, M.V. Chaja, A. Urniezius, S. Butkus, B. Neuenschwander, Machining metals and silicon with GHz bursts: Surprising tremendous reduction of the specific removal rate for surface texturing applications, in: Laser Applications in Microelectronic and Optoelectronic Manufacturing (LAMOM) XXV, International Society for Optics and Photonics, pp. 112670T (2020)
17. G. Bonamis, K. Mishchik, J. Lopez, I. Manek-Hönninger, E. Audouard, C. Honninger, E. Mottay, Industrial GHz femtosecond laser source for high efficiency ablation, in: CLEO: Applications and Technology, Optical Society of America, pp. AM2M.4 (2018)